INTECH
open science | open minds

OPEN ACCESS
ARTICLE

Nanomaterials and Nanotechnology

Electrical transport Features of SiNWs Random Network on Si Support After Covalent Attachment of New Organic Functionalities

Regular Paper

Marianna Ambrico[1,*], Paolo Francesco Ambrico[1] and Rosa di Mundo[2]

1 C.N.R.- Istituto di Metodologie Inorganiche e dei Plasmi, Sezione Territoriale di Bari, c/o Dipartimento di Chimica, Università degli Studi di Bari "Aldo Moro", Italy
2 Dipartimento di Chimica, Università degli Studi di Bari "Aldo Moro", Italy
* Corresponding author: marianna.ambrico@ba.imip.cnr.it

Received 8 March 2012; Accepted 10 April 2012

Abstract Modification of the electrical transport of a random network of silicon nanowires assembled on n-silicon support, after silicon nanowires functionalization by chlorination/alkylation procedure , is here described and discussed. We show that the organic functionalities induce charge transfer at single SiNW and produce doping-like effect that is kept in the random network too. The SiNWs network also presents a surface recombination velocity lower than that of bulk silicon. Interestingly, the functionalized silicon nanowires/n-Si junctions display photo-yield and open circuit voltages higher than those including oxidized silicon nanowire networks. Electrical properties stability in time of junctions embedding propenyl terminated silicon nanowires network and transport modification after secondary functionalization is also shown. These results suggest a possible route for the integration of functionalized Si nanowires, although randomly distributed, in stable large area photovoltaic or molecule sensitive based devices.

Keywords Silicon nanowires, organic functionalization, surface recombination velocity

1. Introduction

Silicon nanowires (SiNWs) have been the subject of an extensive research addressed to explore all their possible applications from the solar energy conversion to sensing. [1-3] SiNWs have been also widely used as building block of the next generation solar cells and high mobility field effect transistors (FETs).[3-8] The advantage of integrating single, arrays or networks of SiNWs in solar cells, is the possibility of decoupling the light absorption from the charge transport of the minority carriers whose lateral diffusion is one order of magnitude lower (hundreds of nm) than that observed in bulk Si (> 1 μm).[6,9,10] Furthermore the enhanced optical absorption from ultraviolet to near infrared optical range could result in a higher efficiency of the Si NW based device. [9]

Recently, the requirement of large scale deposition of silicon nanowires for potential application in microelectronics system like displays, biological and chemical sensors, and also large area solar cells has lead to focus the attention on networks of randomly oriented SiNWs.[1,11,12] Furthermore the lower temperature processing with respect to single Si crystal allows the deposition on plastic flexible substrates.

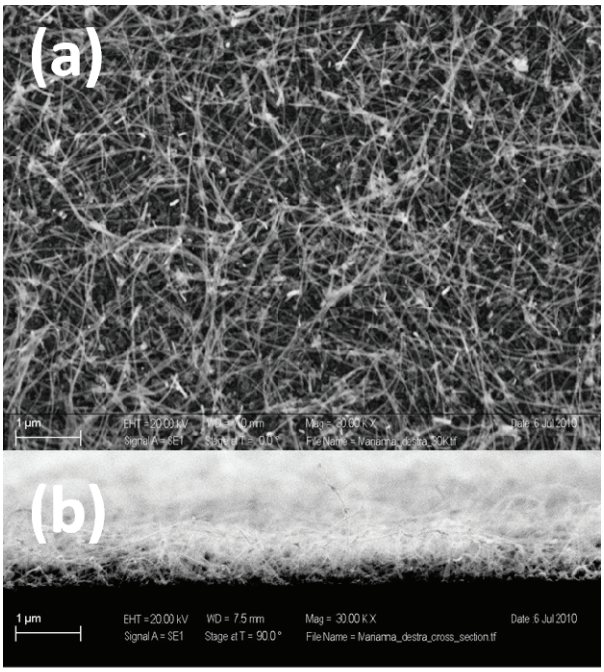

Figure 1. Typical top view and cross sectional SEM images of SiNWs random network on ($N_d \propto 10^{18}/cm^3$) (111) n-Si substrates. SiNWs were prepared by the vapour-liquid-solid (VLS) method using chemical vapour deposition with silane and then terminated with different organic molecules using a chlorination/alkylation process (see ref.15 and 16)

It is noteworthy the observation that in a single SiNW the surface to volume ratio larger than in Si bulk, although advantageous, implies that the surface states as dangling bonds, defects or adsorbates play a more relevant role that could affect the device performances. Also, the silicon dioxide (SiO_2) coating SiNWs is thought to induce trap states at the SiO_2/Si interface increasing surface carrier recombination. [13] This has been shown to limit, for example, the possibility of controlling the channel conductivity in SiNWs based FET devices. [7] The use of H terminated SiNWs gave results unstable in time due to subsequent oxidation under air exposure. [13] However, the high SiNWs surface reactivity allows their chemical manipulation resulting in a desired change of transport properties. [14] With respect to H and SiO_2 terminated–SiNWs, non-oxidized methyl (CH_3-) terminated SiNWs displayed increased mobility and allowed to achieve FET devices on-off ratio higher than 10^5 together with chemical stability in time.[15] Although CH_3 termination is quite stable in air and ensure a good coverage of the top Si atoms, subsequent bonding of organic functionalities is not allowed. Recently, intrinsic (undoped, 10^{15}-10^{16} cm^{-3}) SiNWs have been covalent bonded via Si-C to different molecules (methyl, propenyl and propynil) by chlorynation/alkylation processes. Specifically, it has been shown that propenyl scaffold lead to both full coverage of the Si sites and are capable of further functionalization. [15,16]

This work aims to enlighten on the electrical transport properties of junctions built with a random network of the above mentioned functionalized SiNWs (RN-SiNWs) self assembled on a silicon support. Evidence of the further carrier transport modification across a similar junction including random network of subsequently functionalized propenyl –SiNWs is also presented.

2. Experimental

2.1 Si NWs fabrication

The SiNWs random network under investigation have been prepared on highly doped n-Si(111)(Sb doped, $10^{18}/cm^3$) starting from intrinsic SiNWs (10^{15}-10^{16} $/cm^3$) prepared by vapor-liquid-solid growth mechanism using chemical vapour deposition with silane. After being cleaned (N_2 flow), hydrogen-terminated Si samples were prepared by etching the amorphous SiO_2 coating, then exposing the SiNWs to buffered HF solution (pH=5) for 40 s. The samples were then removed and rinsed in water to limit oxidation, dried in flowing N_2(g) for 10 s, and immersed into a saturated solution of PCl5 (99.998%, Alfa Aesar) in C_6H_5Cl (0.65 M) that contained a few grains of $C_6H_5OOC_6H_5$ to act as a radical initiator. The reaction solution was heated at 90±10 °C for 10 min. The chlorinated samples were rinsed with tetrahydrofuran (THF) and the samples were transferred to a N_2-purged glove box. While being in the glove box, the chlorinated samples were immersed for 12-24 hrs (in the case of Si NWs) in a THF solution of 3.0 M methylmagnesium chloride (CH_3MgCl) at 120±10 °C, 0.5M 1-propenylmagnesium bromide (CH_3-CH=CH-MgBr), or 0.5 M 1-propynylmagnesium bromide (CH_3-C≡C-MgBr) for producing alkyl terminated Si samples. Alkylated samples were either: (i) rinsed with THF, methanol and transported out of the glove box and further rinsed with DI water, and dried under a stream of N_2(g); or (ii) sonicated for ca. 10 min in the same solutions and dried under a stream of N_2(g). The alkylation process was gentle in the sense that it neither damaged (or broken) the Si samples nor changed the dimensions of as-grown Si NWs. The subsequent propenyl-Si NWs functionalization with photoactive aryldiazirine cross-linker (TDBA-OSu) was performed by placing functionalized SiNWs in a 10-mm quartz cuvette. Then the solution was added and

immediately illuminated with a broadband UV lamp. The samples were then rinsed vigorously with CCl_4, CH_2Cl_2, and water. The Para-Phenylenediamine (PPD) deposition on TDBA-OSu-CH2-CH=CH-Si NW was performed by placing the TDBA-OSu-CH2-CH=CH-Si NW in a solution of *para*-phenylenediamine (PPD) in DMF. After immersion for 2 h, the samples were cleaned by rinsing with DMF and CH_2Cl_2, and dried by N_2(g) flushing.[15,16]Figure 1(a-b) displays a typical top view (1a) and cross sectional scanning electron micrograph (1b) of a SiNWs random network fabricated on the n-Si substrate. The average SiNWs length, roughly corresponding to the thickness of the SiNWs random network, was estimated around 2 μm, while the single SiNW had an estimated average diameter of 50 nm.

2.2 Electrical measurements set up

A typical configuration for electrical characterization on functionalized RN- SiNWs on nSi is displaced in the Figure 2. A gold slab (2x2 mm^2) has been mechanically placed on the top of the random network and used as top contact to avoid any effect of gold contact evaporation on NWs (e.g. gold penetration in the random network), as well as some possible damage on organic termination

The dark current (*J*) and photocurrent (J_{ph}) characteristics as a function of the applied bias *V* (*J vs V*, J_{ph} *vs V*) were collected in air and at room temperature by using an electrometer and a voltage supplier. The open circuit voltage values V_{oc} have been extracted from J_{ph} *vs V* curves too. The photo-efficiency conversion Y_{ph} of the devices was measured by detecting the short circuit current using the electrometer during a t=60 s continuous white light pulse provided by a 70 W halogen lamp (power density of 100 mW/cm^2). The Y_{ph} *vs t* values have been determined for each structure by subtracting the corresponding dark current density J_{dk} (i.e.current detected before light on) from the total short circuit current J_{sc} and then by normalizing to the dark current density i.e. $Y_{ph}= (J_{sc}- J_{dk}) / J_{dk}$. It is worth remarking that the negative value of the detected current at zero bias, confirms the presence of a photovoltaic behaviour in the full set of the examined devices.

A mapping of the junction *J vs V* (*J*, dark current), J_{ph} *vs V* (J_{ph}, photocurrent) characteristics, open circuit voltage, V_{oc} and photo-efficiency Y_{ph} *vs t*, has been performed by placing the gold slab at different positions on the NWs layer surface. This procedure allowed to evaluate both the uniformity of organic molecule termination effect on RN-SiNW on the junction transport properties and to account for the SiNWs surface density on silicon support. The reported *J vs V*, J_{ph} *vs V*, Y_{ph} *vs t* curves and V_{oc} values results therefore from the average of the values extracted from the collected characteristics at the different positions of the Au slab.

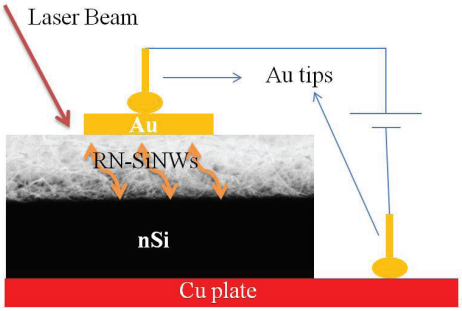

Figure 2. Schematic of the device configuration used for optoelectronic characterizations. A gold slab has been used instead of evaporated gold while InGa past has been painted on the back side of n-Si wafer for ohmic contact formation. The orange arrows is a simplified representation of the current percolation paths.

The transient photoconductivity measurements have been performed by using the contact configuration shown in Fig. 2 and using the λ=590 nm of a pulsed Dye laser light (repetition rate 10 Hz, τ=9ns, energy of tenths of nJ per pulse, laser spot diameter 2 mm). The laser has been gently focused onto the SiNWs random network side in a region very close to the Au slab. This position has been chosen in order to avoid laser screening or reflectance effects due to the Au slab. The J_{ph} signal is measured at zero bias in mV on the 1 MΩ input resistance of a Lecroy digitizing oscilloscope. The data have been then normalized to the maximum detected current and the decay times (τ) have been obtained by the exponential fit of the photoconductivity signal averaged over 1000 shots.

3. Results and discussion

Figure 3 shows the comparison between the averaged *JvsV* characteristics performed on RN of (SiO_2-SiNWs)/n-Si and on RN of functionalized SiNWs/nSi junctions.

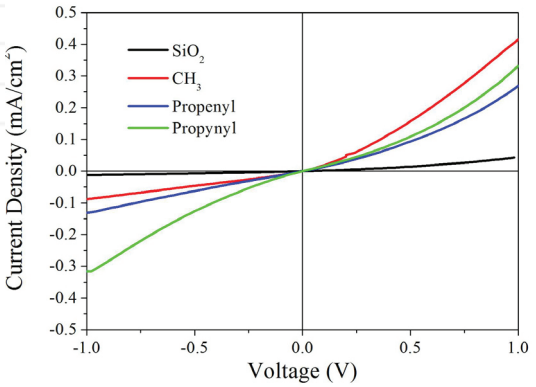

Figure 3. *JvsV* characteristics collected on RN of SiO_2 and molecularly functionalized SiNWs array on n-Si junction .

The good packing density of the SiNWs, also evidenced by SEM analysis, can be further deduced by the decrease of the detected current across the junction of around two

orders of magnitude with respect to that measured under the same experimental conditions (Au slab) on bare degenerated n-Si (data not shown). Interestingly, a general increase of the forward current has been detected for junction embedding functionalized SiNWs RN compared to those including SiO_2- SiNWs ones. The results furthermore show a slightly higher rectification ratio in junction embedding methyl and propenyl terminated SiNWs RN, rather than in those including propynil -SiNWs RN.

For all the structures embedding RN-SiNWs, the averaged forward bias *JvsV* characteristics display a power law dependence J *vs* V^n with $1.4<n<2$ depending on the molecular terminations. Therefore, a percolative mechanism is responsible for the conducting path across the SiNWs sandwiched between the top and bottom electrode [17,18]. Specifically, the n-value goes from that of a super-linear regime (1.4, for CH_3-SiNW) to that typical of a space charge limited current (2, for SiO_2 and propynil -SiNWs). Moreover, other interesting features in *JvsV* junction characteristics can be observed.

In particular, in the as received molecular modified RN SiNWs/n-Si junction the increase of forward current with respect to RN SiO_2-SiNWs/n-Si one is associated with a current onset displacement toward lower voltages. This effect, that is present notwithstanding the similar SCLC behaviour (n~2) is typically observed in single nanowires when terminated with positive dipolar molecular layer. [19,20] The positive dipole formation could be one of the effects of functionalization on each single NWs producing a charge transfer such as an electron donation from the SiNWs to the molecule.[20] This effect is due to a decrease of the electron carrier concentration and then a downward shift in the SiNWs Fermi level position. Conversely, this implies a modification from intrinsic-like to a more p-type-like character of each NW. [20] Interestingly, the molecule termination effect is detectable also when SiNWs are arranged in a random network probably because of the high SiNW density. As a matter of fact, the p-type character of the molecularly functionalized SiNWs RN is also clearly evidenced by the increase of the junction rectification ratio compared to that encountered in the junction embedding the SiO_2-SiNWs RN . The latter behaviour can be ascribed to the similar n-like character of the network and n-Si support.

However, the current onset displacement (indicating the magnitude of the p-type doping of SiNWs network) does not strictly follow the increase of the theoretical dipole of SiNW molecular termination. In fact even if the dipole values are 0.8D, 1.3D and 1.6D for methyl-Si, propenyl-Si and propynyl-Si respectively, the highest increase in conductivity (i.e. high p-doping like effect) has been observed in methyl terminated SiNWs.[21] The effect of the different molecular coverage of the single SiNW can be excluded, since previously reported results evidenced a nearly full molecular coverage (around 100%) for all the terminations. [15] Another possible factor reducing the current across the propenyl and propynyl -SiNWs layer could be the different tunnelling effect from the SiNWs across the molecular layer due to thickness higher than that of CH_3- (2.3 Å, 5.3 Å and 5.8 Å for methyl, propenyl and propynil termination respectively).[15] However even if *JvsV* data are scaled to account for tunnelling effect, the trend is preserved when changing the molecule termination. Also, interface oxidation effect can be excluded since oxide on functionalized SiNWs has been detected after around 10 days and 20 days in methyl and propynyl samples respectively, while it does not occur at all in propenyl.[15] It is noteworthy to observe that in case of small NWs (50 nm diameter) dimensionality implies that surface states can strongly affect the molecule-SiNWs charge transfer effect so that mechanisms like pinning of the Fermi level at different position in the SiNWs band gap could affect the carrier transport properties. [22] Therefore, the fact that the current onset shift in propenyl and propynyl-SiNWs is lower than that in methyl-SiNWs could be explained by hypothesizing the presence of a different energy distribution of the interface states across the SiNWs gap.[22]

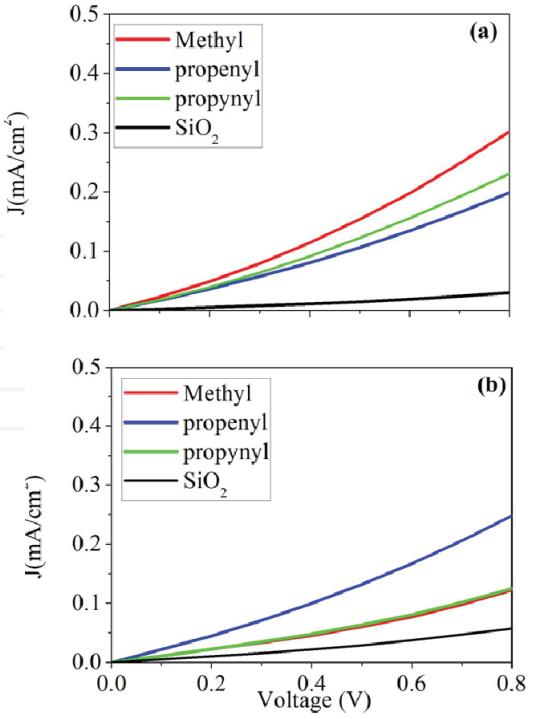

Figure 4. Dark forward current density vs. voltage (*J vs. V*) characteristics of RN SiNWs/n-Si junction; in the legend the corresponding SiNWs terminations have been indicated. a) *J vs.V* collected soon *a*fter receiving the samples (around four days after sample preparation); b) *J vsV* characteristics collected one month later.

If this is the case, the molecule- SiNWs charge transfer effect can be limited due to the interface state density causing the pinning of the Fermi level position inside the NWs gap. As a further limiting factor of charge transfer, the different electrical field screening effect of propenyl and propynyl-SiNWs compared to methyl-SiNWs has to be taken into account. This effect can decrese the external applied electric field across the NWs leading to a reduced value of the detected current. The reason of the observed behaviour can be clarified through the examination of surface recombination velocity results below reported.

The electrical transport stability across the functionalized RN-SiNWs/nSi junction was checked by performing *JvsV* as soon as the samples were received (about 10 days after sample preparation) (Figure 4(a)) and one month later (Fig.4(b)) under the same experimental conditions.

The *JvsV* characteristics collected after one month (Fig. 4b) show that the voltage shift of the current onset observed in propenyl –SiNWs/n-Si with respect to SiO_2-SiNWs/pS, is almost the same, while it is reduced in methyl and propynil- SiNWs/n-Si. These data confirm what already observed about the high resistance to oxidation of the propenyl-SiNWs; here we also show that also the dipole induced doping-like effect is preserved[15]

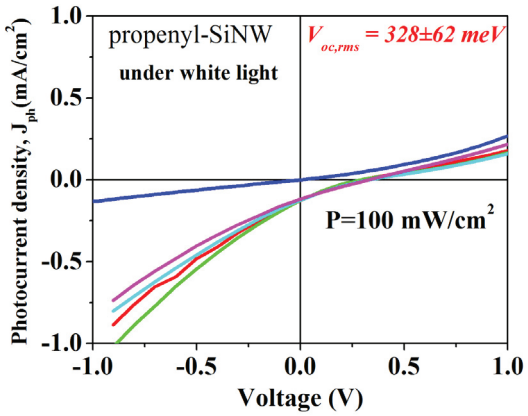

Figure 5. Photocurrent density vs Voltage (J_{ph} *vs* *V*) characteristics collected under white light illumination on propenyl functionalized SiNWs/nSi junction at four different positions of the gold slab on top of the junction. The average $V_{oc,rms}$ value has been found $V_{oc,rms}$ =328±62 meV. The corresponding averaged dark current density vs voltage has been inserted for comparison

Figure 5 shows the photocurrent density vs. voltage (J_{ph}*vs*V) related to the propenyl-SiNWs/n-Si junction along with the dark *JvsV* curve. The detection of the open circuit voltage V_{oc} and short circuit current indicates the presence of a photovoltaic behavior of the junction. We need to highlight that the Au/nSi junction did not show a photovoltaic behavior (no open circuit voltage was detected) as a consequence of the high silicon dopant concentration. In Table 1 the resulting averaged V_{oc} values for the full set of samples are summarized. Values of fill factor and efficiency have not been reported since we worked by using a non-optimized contact configuration. This can be deduced by the collected J_{ph}*vs*V value strongly influenced by shunt and series resistance effect, which insted do not affect the observed V_{oc} values. The V_{oc} values of SiO_2-SiNWs /n-Si have been found higher than those of SiNWs cells deposited on stainless steel.[1] The comparison between photovoltaic parameters including RN of junction of SiO_2-SiNWs and those observed on functionalized SiNWs allows to appreciate a V_{oc} increase higher than 100 mV on propenyl and propynyl –SiNWs while that observed in methyl-SiNWs does not show significant changes.

Furthermore, for all measurements, slight scattering in the short circuit photocurrent densities (J_{sc}) values have been found when changing the Au slab position on the SiNWs random network. The observed V_{oc} increase in can be explained by considering that in a semiconductor the V_{oc} magnitude is typically determined by the competition of diffusion and recombination processes. This relies on the Shockely diode equation, below reported. [23,24].

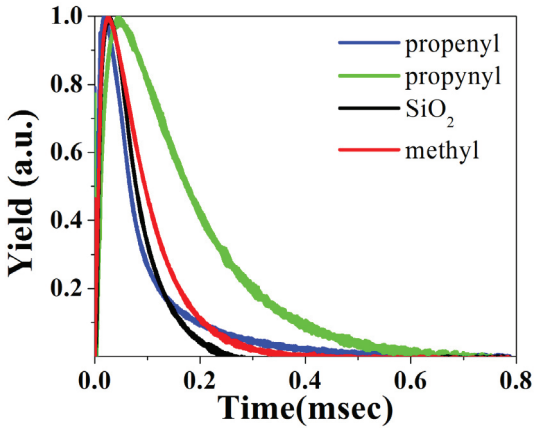

Figure 6. Time resolved photoconductivity decays of SiO_2 and functionalized RN SiNWs/nSi junction. A single exponential fit yields increasing value of time constant (93 μs and 142 μs) respect to SiO_2 termination (37 μs) with a corresponding reduction of surface recombination velocity (see Table 1).

$$V_{oc} \propto \ln(J_{sc} L_p N_d /(q D_p n_i^2)) \quad (1)$$

where L_p is the minority carrier (hole) diffusion length; N_d the majority carrier dopant density, D_p is the minority carrier diffusion coefficient, n_i the intrinsic carrier concentration. Moreover:

$$L_p/(D_p)^2 = \tau_{eff} \quad (2)$$

where τ_{eff} is the minority (hole) recombination time including bulk and surface contribution as

$$1/\tau_{eff} = 1/\tau_{bulk} + 1/\tau_s \sim \tau_s \quad (3)$$

being τ_s =d/2S, where d is the sample thickness and S is the surface recombination velocity. Therefore, the higher the recombination time (i.e. the lower the surface recombination velocity), the higher the V_{oc}.Similarly, we attributed the V_{oc} formulation to the RN-SiNWs/n-Si junction where the thickness d is represented by the nano-wire length (also corresponding to the estimated average thickness of the RN). According tothese hypotheses, the observed increase of V_{oc} has to be ascribed mainly to variations ofsurface recombination velocity and to the increasing p-type-like behaviour of the RN-SiNWs due to charge transfer effect. Figure 6 shows the photocurrent decays of SiO_2-SiNWs and methyl, propenyl and propynil –SiNWs/n-Si junctions. It can be observed that the these decays are due to the effect of the charge transport across SiNWs random network. In fact, the measurements performed on bare n-Si under the same illumination conditions returned a decay time one order of magnitude lower.[25] The recombination velocities are collected in Table 1. Here we also compare surface recombination velocities, S, obtained on methyl and octylate terminated n-type silicon surface.[26] Values of S = 0.7 cm s^{-1} have been extracted in RN of propenyl and propynyl –SiNWs, i.e. around four and one half lower than that of RN-SiO_2 (2.7 cm s^{-1}) and methyl (1.3 cm s^{-1}) –SiNWs, respectively. The observed reduction of surface recombination velocity agrees with analogous effects seen on chlorinated/alkylated nSi surfaces.[26] In propenyl –SiNWs films a fast decay component (3.7 cm s^{-1}) has been also observed. The reduction of the S values with respect to SiO_2 RN–SiNWs indicates that molecule terminations partially passivate interface trap states, explaining this way the achievement of stability to oxidation. Since the surface recombination velocity is directly correlated to the interface state density, it can be deduced that the passivation is more effective in the propenyl and propenyl terminated SiNW rather than in the methyl terminated one. Furthermore, the observed lower current in junction embedding propenyl and propynil terminated SiNW RN (Fig.4a) should be ascribed to a molecule induced higher electric field screening effect, rather than to an interface states induced pinning effect.

Fig. 7 shows the *JvsV* characteristics across the RN-propenyl- SiNWs/n-Si after a subsequent covalent attachment at propenyl-SiNWs of TDBA for two different illumination time of a 365 nm broadband UV lamp [15,16]. It can be observed that the carrier transport across the propenyl-SiNWs/nSi junction is strongly affected by TDBA covalent attachment and is represented by a large increase of forward current level and rectification.

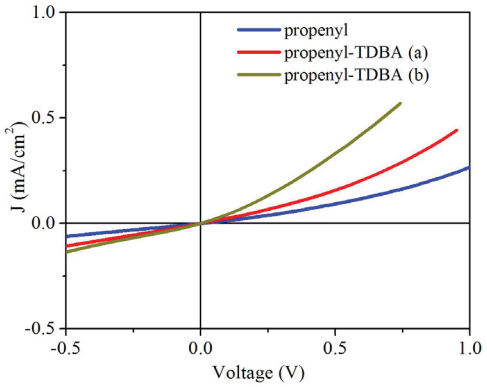

Figure 7. Current density vs voltage (*JvsV*) characteristics after second functionalization of RN propenyl terminated-SiNWs/n-Si junction by: (a) propenyl-TDBA and (b) propenyl-TDBA for 10 and 30 min 365 nm broadband UV lamp illumination respectively (see ref. 13-14). The *JvsV* of the RN propenyl–SINWS/n-Si junction has been reported for comparison. The measurements on propenyl-TDBA (30 min) has been stopped at a forward bias 0.5 V level due to detected current higher than the maximum detectable by the electrometer (> 20 mA)

Silicon structure	$V_{oc,rms}$ *(meV)*	*S (cm s^{-1})*
SiO_2-nSi bulk*	-	>20
CH_3-nSi bulk*	-	17
Clorinated/alkylated-nSi bulk*	-	21
SiO_2-RN-SiNWs	243	2.7
CH_3-RN-SiNWs	238	1.3
Propenyl-RN-SiNWs	328	0.7-3.6
Propynyl-RN-SiNWs	370	0.7

* from ref.25

Table 1. Open circuit voltages (V_{oc}) and surface recombination velocities obtained on functionalized RN SiNWs/nSi junctions by current versus voltage under light irradiation ($J_{ph}vsV$) and exponential fitting of time resolved photoconductivity respectively. The RN SiNWs average length, d, used for S calculation was estimated of around 2 μm from SEM images.

Figure 8a reports the photoyield as a function of time at zero bias of RN of methyl-, propenyl and propynyl terminated SiNWs/nSi. A sharp response to light on-off with values higher than those observed in SiO_2-SiNWs RN can be observed. Moreover, the photocurrent densities observed in propynyl and propenyl terminated SiNWs/pSi junctions have been found lower than those observed in CH_3- SiNWs/pSi. The covalent attachment (Fig. 8b) of TDBA on propenyl-SiNWs produces also a photocurrent density higher than that of propenyl. The increase of the short circuit current, J_{sc} ,of the junction could be related to the different light power absorbed by the functionalized SiNWs layer. This is thought to be due to a lower light screening effect (i.e. lower reflectance) when linking propenyl to TDBA, thus reducing the RN SiNWs light power absorption. [9,27]

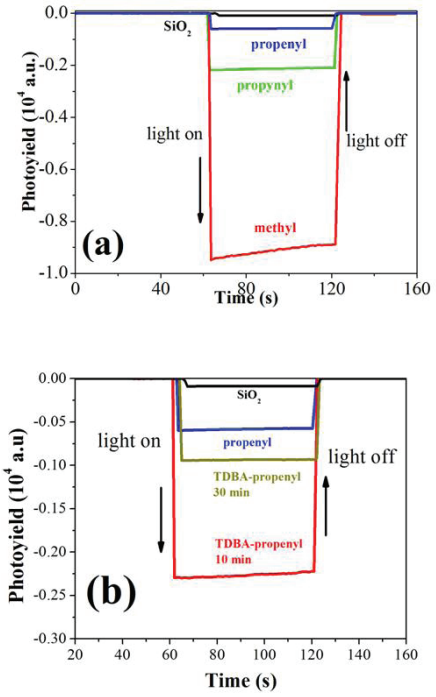

Figure 8. DC photo-yield vs. illumination time (Y_{ph} *vs.* t) collected at zero bias: **(a)** on SiO_2 and functionalized SiNWs/n-Si junction under 60 s white light illumination (AM 1.5, 100 mW cm^{-2}). **(b)** On RN propenyl-SiNWs/n-Si junction before and after further functionalization steps by TDBA molecules for 10(a) and 30 (b) minutes UV broadband lamp exposure (see ref 15, 16).

4. Conclusions

This work provides new insights into electrical transport and optoelectronic behaviour of junctions formed by random network of SiNWs on n-Si, where single SiNWs are coupled with new organic functionalities. The observed decrease of surface recombination velocity indicates that the carrier transport characteristics across the junction are affected by the organic functionalities. Moreover, the effect of passivation of interface traps by propenyl functionalization of oxidized SiNWs is transferred also in the SiNWs RN, as can be desumed by the achieved stability of the electrical response of the RN based on propenyl-SiNWs. Finally, the modification of carrier transport after subsequent covalent attachment of new organic functionalities suggests the possibility of tailoring new stable large area hybrid molecule-SiNWs based devices, suitable for specific molecule sensing.

5. Acknowledgements

The authors acknowledge Dr. H. Haick and Dr. O. Assad of the The Department of Chemical Engineering and Russell Berrie Nanotechnology Institute, Technion - Israel Institute of Technology for sample preparation.

6. References

[1] Tsakalakos L., Silicon nanowire solar cells *Appl.Phys.Lett*. 2007, 91,233117

[2] Kolmakov A., Layer-by-Layer Assembly of Nanowires for Three-Dimensional, Multifunctional Electronics, *Nano Lett.* 2007,7,773

[3] Jie J., Surface-Dominated Transport Properties of Silicon Nanowires, *Adv.Funct.Mater.*2008,18,3251

[4] Peng K., Silicon nanowire array photoelectrochemical solar cells, *Appl.Phys.Lett.2008,92,163103*

[5] Stelzner Th., Silicon nanowire-based solar cells, *Nanotechnology 2008,*19,295203

[6] Kelzenberg M.D., Photovoltaic Measurements in Single-Nanowire Silicon Solar Cells, *Nano Lett.2008*,8,710

[7] Cui Y., High Performance Silicon Nanowire Field Effect Transistors, *Nano Lett.* 2003,3,149

[8] Briseno A.L., Fabrication of Field-Effect Transistors from Hexathiapentacene Single-Crystal Nanowires, *Nano Lett.*2007,7,668

[9] Tsakalakos L. Strong broadband optical absorption in silicon nanowire films, *Jnl. of Nanoph 2007*,1,013552

[10] Hu L., Analysis of Optical Absorption in Silicon Nanowire Arrays for Photovoltaic Applications, *Nano Lett 2007,7,3249*

[11] Duan X., High-performance thin-film transistors using semiconductor nanowires and nanoribbons, *Nature 2003, 425, 274*

[12] Heo K., Large-Scale Assembly of Silicon Nanowire Network-Based Devices Using Conventional Microfabrication Facilities *Nano Lett., 2008,8,4523,*

[13] Sham T.K., Electronic structure and optical properties of silicon nanowires: A study using x-ray excited optical luminescence and x-ray emission, *Phys.Rev.B 2004,70,045313*

[14] Haick H., Electrical Characteristics and Chemical Stability of Non-Oxidized, Methyl-Terminated Silicon Nanowires, *J.Am.Chem.Soc.2006,128,8990*

[15] Puniredd S.R., Highly Stable Organic Monolayers for Reacting Silicon with Further Functionalities: The Effect of the C–C Bond nearest the Silicon Surface, *J. Am. Chem. Soc. 2008, 130,* 13727

[16]Assad O., Stable Scaffolds for Reacting Si Nanowires with Further Organic Functionalities while Preserving Si-C Passivation of Surface Sites, *J.Am.Chem.Soc.* 2008,130,17670

[17] Hunt A., Relevance of percolation theory to power-law behavior of dynamic processes including transport in disordered media, *Complexity* 2009,15, 13

[18] Stavarache I., Percolation phenomena in Si-SiO2 nanocomposite films, *J. Optoelectron. Adv. Mater.* 2007, 9, 2644

[19] Haick H., Controlling Semiconductor/Metal Junction Barriers by Incomplete, Nonideal Molecular Monolayers, *J. Am. Chem. Soc.*, 2006, *128* ,6854

[20] Haight H., Controlling the Electronic Properties of Silicon Nanowires with Functional Molecular Groups, *Nano Lett.*, 2009, 9, 3165
[21] Haick H., private communication
[22] Bashouti M.Y., Controlling the Electronic Properties of Silicon Nanowires with Functional Molecular Groups, *Small* 2009,5,2761
[23] Shockley W. in *Electrons and Holes in Semiconductors* (Ed:Van Nostrand, New York, 1950) p.318
[24] Royea W.J., Fabrication of minority-carrier-limited *n*-Si/insulator/metaldiodes,*Appl.Phys.Lett*.1990,56,1919
[25] Royea W.J., Preparation of air-stable, low recombination velocity Si(111) surfaces through alkyl termination, *Appl.Phys.Lett*. 2000,77,1988
[26] Tyagi, M. S., Overstraeten, Minority carrier recombination in heavily-doped silicon, *Solid State Electron.* 26, 6 (1983) 577-598.
[27] Garnett E.C, Light Trapping in Silicon Nanowire Solar Cells, *Nano Lett*. 2010,10,1080